STUDY OF THE STRUCTURE OF ULTRATHIN SILICON DIOXIDE FILMS

A.A. EVTUKH, I.P. LISOVSKII, V.G. LITOVCHENKO, A.YU. KIZJAK, YU.M. PEDCHENKO, L.I. SAMOTOVKA

Lashkarev Institute of Semiconductor Physics, Nat. Acad. Sci. of Ukraine
(41, Nauky Prosp., Kyiv 03028, Ukraine)

UDC 621.382
©2006

The structural properties of ultrahin (2—10 nm) and thin (10—40 nm) SiO_2 films grown thermally on silicon at $T = 800 \div 950$ °C in oxygen atmosphere were investigated in detail with the help of three independent analytical methods, namely, IR spectroscopy, ellipsometry, and step-by-step chemical etching. We discovered a wide transition layer of SiO_2 adjacent to silicon. The transition layer between silicon and bulk SiO_2 is heterogeneous and consists of three layers. There exists a transition SiO_x layer between Si and SiO_2 approximately 1.5 nm in thickness. A SiO_2 film is also heterogeneous and consists of two layers. The first one has a thickness d of 2—3 nm, and $d > 8$ nm for the other one. Between these two layers, there exists a transition layer 3—5 nm in thickness.

1. Introduction

Silicon dioxide films usually grown on silicon using the method of thermal oxidation create an interface with low density of interface states. In addition, SiO_2 films are characterized by a high resistivity ($\sim 10^{15}$ $\Omega\times$cm), wide band gap (∼9 eV), and high melting temperature (1718 °C) [1]. These unique properties of silicon dioxide films have promoted the revolutionary development of silicon-based micro- and nanoelectronics. A field-effect transistor based on a metal–oxide–silicon (MOS) structure represents a basic structural part of any integrated circuit (IC).

A Si/SiO_2 interface is the most important part of MOS structures. A continuous scaling down of an IC chip is accompanied with an improvement in the operating speed of circuits, memory size, and the cost per bit. According to the scaling rules, the continuous miniaturization of devices requires the corresponding reduction of the thickness of a gate oxide layer. For small transistors, the thickness reduction of the oxide layer is necessary for obtaining a high drive current and avoiding the short channel effects. In order to effectively control the channel current, MOS-based submicrometer devices must have a high capacity. As the capacity is inversely proportional to the thickness of a dielectric, it is necessary to decrease the thickness of SiO_2 in devices of submicro- and nanoelectronics. Therefore, the thickness of the gate dielectric SiO_2, that amounted to hundreds of nanometers 40 years ago, has been decreased to less than 2 nm by now [2, 3]. The forecasts of the International Technology Roadmap for Semiconductors [3] show that, in the nearest 5 years, there will be a need in the gate dielectric SiO_2 having 1 and less nanometers in thickness.

In addition to CMOS IC, ultrathin SiO_2 films are also widely used in elements of electrically programmable memory [4]. The processes of tunnel transport of charge carriers through a thin film allow one to write and erase the charge. The energy barriers created by SiO_2 are also responsible for the charge storage in memory elements. A further decrease of the size of memory elements leads to the creation of a monotransistor memory element with a change in the threshold voltage at reprogramming by approximately 0.25 V, which corresponds to the storage of one electron in a separate nanocluster of a SiO_2(Si) nanocomposite film [4—7]. In such nanostructures, the quantum-size effect and the direct tunneling are realized. The usage of ultrathin SiO_2 films in devices of submicro- and nanoelectronics makes strict demands of their properties such as uniformity, high strength of the breakdown electric field, and resistance to the injection of hot electrons at high electric fields (higher than 3×10^6 V/cm) [8].

In the case of ultrathin SiO_2 films, the Si/SiO_2 interface becomes a more critical and restrictive part of a gate dielectric. In spite of the great attention that was continuously paid by researchers to the investigation of SiO_2 and Si/SiO_2 interfaces, there still exist some unsolved physical problems, especially, in the case of ultrathin SiO_2 films [1, 9].

In our previous papers, the so-called three-layer model of the Si—SiO_2 system has been developed [10, 11]. It takes into account the existence of an intermediate layer having several nanometers in thickness between crystalline silicon and bulk amorphous SiO_2. This layer contains a sublayer of imperfect oxygen-enriched silicon

from the side of the Si substrate and a transition SiO_x sublayer ($0 < x < 2$) from the side of SiO_2. The parameters of the transition SiO_x sublayer, namely its thickness, the band gap, height of energy barriers, and effective masses of electrons and holes were investigated and determined for some technologies in our work [12]. In addition, it is known that IR-spectroscopy gives a good possibility to observe the structure of the transition layer between silicon and a bulk amorphous SiO_2 film. As was shown in our works [l3,14], the transition layer is significantly thicker than the SiO_x gap.

In this paper, the results of studies of the structure of ultrathin SiO_2 films are described. We made use of some analytical methods, namely IR spectroscopy and ellipsometry along with chemical etching. The obtained experimental results confirm the existing model of the layer structure of SiO_2 thin films and explain some details of the thickness dependence of structural properties.

2. Experiment

We made use of n- and p-silicon wafers 100 mm in diameter, with (100) and (111) orientations and the doping levels of 1×10^{15} and 3.5×10^{14} cm^{-3}, respectively. Wafers of different types were simultaneously oxidized in a furnace. First, after RCA cleaning, sacrificial oxide films (80—100 nm) were grown on the silicon wafers in the O_2 atmosphere at 1000 °C with the following ten-minute annealing in N_2 at the oxidation temperature. After that, these films were removed in a water solution of HF. A stable hydrogen passivation of the silicon surface can be obtained after etching the oxide layer in diluted HF and rinsing in water [15]. Then the investigated ultrathin (2—40 nm) gate oxide layers were grown on clean silicon wafers by means of the thermal oxidation in furnaces of the conventional type. The thermal oxidation was performed in dry O_2 at temperatures of 800 — 950 °C. The wafers were introduced in a furnace in the O_2 environment as well.

The oxide thickness was measured with the help of a laser ellipsometer ($\lambda = 632.8$ nm) at 5 points on the wafer. We determined the thickness dependence of the real part of the refractive index at the successive etching of SiO_2. The errors arising in the determination of n and d amounted to ±0.003 and ±0.1 nm, respectively. The thicknesses of initial SiO_2 films before the step-by-step etching were equal to 20—40 nm.

IR transmission spectra (at the normal and oblique 70° incidences of IR light) were measured in the range of wave numbers 900—1400 cm^{-1} for both Si—SiO_2 and Si (after the removal of the oxide layer) samples. Then the absorbance A of the oxide layer was calculated. The deconvolution of the absorption band into Gaussian profiles and their relation to the oxide structure were described earlier [13, 14]. We determined their number and basic parameters (the position of the maximum W, its full width at half maximum (FWHM) H, and area S). The accuracy of the deconvolution was characterized by a roof-mean-square deviation of the summed Gaussian profiles from the experimental spectrum and did not exceed 2×10^{-2}.

The data reported in [16, 17] for two oxide films (3 and 10 nm) were also analyzed. The obtained number of Gaussians, positions of their maxima, and FWHM values were practically the same as those obtained for our samples. This fact indicates that the results of the deconvolution are rather unambiguous and general and don't depend on the preparation of samples or the oxidation procedure.

3. Results and Their Discussion

I R - s p e c t r o s c o p y. IR-spectroscopy is an effective tool for investigating the microstructure of silicon oxide films. One usually analyzes the position of the principal absorption band, which is conditioned by Si—O stretching vibrations. It is located within the range of 1000—1100 cm^{-1} depending on the oxide content, its density, and porosity, as well as the water contamination [18—27]. Thus, such an analysis enables one to make certain conclusions concerning the quality of oxide. However, the capability of the IR technique was recently shown to be much wider [13,23,25]. In particular, it allows one to determine the structural arrangement of oxygen in a SiO_x lattice ($0 < x < 2$), i.e. to estimate the parameters of the middle- and short-range order of the lattice of vitreous silicon dioxide and nonstoichiometric silicon oxides, respectively [25]. It is achieved by using the mathematical analysis of the form of the principal absorption band. As a rule, it may be done by the decomposition of this band into Gaussian profiles and the further analysis of their parameters in the framework of the Random Bonding Model. In particular, the positions of the peaks of elementary components enable one to calculate the corresponding values of Si—O—Si bond angles and to describe them with certain kinds of rings (SiO_2) formed by SiO_4 tetrahedra or SiO_ySi_{4-y} molecular clusters (SiO_x with $x < 2$). Such an approach was successfully used earlier for studying the structure of SiO_2 films (with the thickness of films lying in the

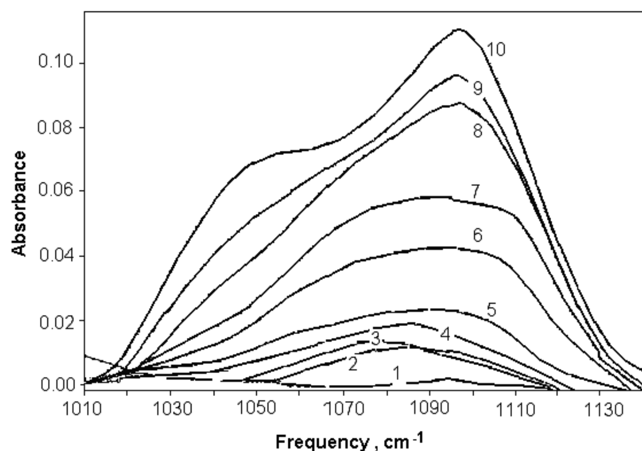

Fig. 1. Principal IR absorption bands of ultrathin SiO_2 films having a thickness d of: (nm) *1* — 0.5; *2* — 3; *3* — 5; *4* — 8; *5* — 10; *6* – 13; *7* — 19; *8* — 25; *9* – 31; *10* — 40

range 7—100 nm) [13, 14, 25]. In this work, we apply it to the investigation of thinner SiO_2 films.

The typical IR spectra obtained for oxides of various thicknesses are shown in Fig. 1. One can see that the intensity of absorption and the position of the peak of the absorption band depend on the oxide thickness. The dependence of the position of the maximum $\nu_{\rm m}$ of the absorption band on the oxide thickness is shown in Fig. 2,*a*. As is seen, this dependence is nonmonotonous. The configurations of SiO_4 tetrahedra in a random continuous network for some thicknesses of SiO_2 films are demonstrated in Fig. 2,*b, c*. A part of the thickness dependence of the position of the IR absorption peak for the case of thinner oxides is shown in Fig. 3. Here we also show the results obtained in [22]. The agreement of our data and those of [22] is rather good, but a more detailed thickness dependence obtained in our case reveals the nonmonotonous character of the thickness dependence of the peak position: the minimum value of $\nu_{\rm min}$ is achieved for films with an oxide thickness of approximately 7 nm, i.e. in the thickness range, where some peculiarities in the behavior of the growth kinetics and electrical characteristics were observed [21]. The given data enable one to make another conclusion. In [21], a monotonous increase in $\nu_{\rm m}$ with thickness $d_{\rm ox}$ ($3 < d_{\rm ox} < 50$ nm) was proved to be associated with the interference, but nonmonotonous variations in the $\nu_{\rm m}(d_{\rm ox})$ dependence cannot be explained by this effect. Hence, such a feature should be related to structural transformations that take place during the oxide growth. Such a conclusion is verified by the results of the analysis of the form of the absorption band.

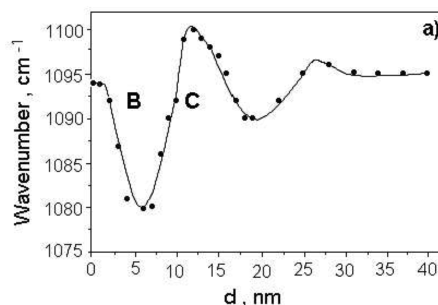

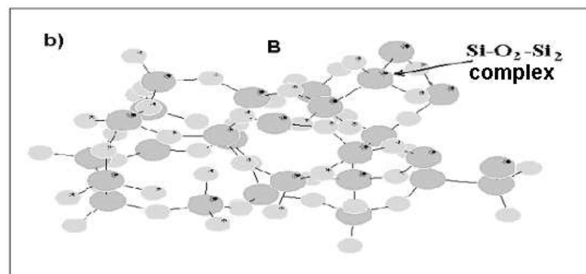

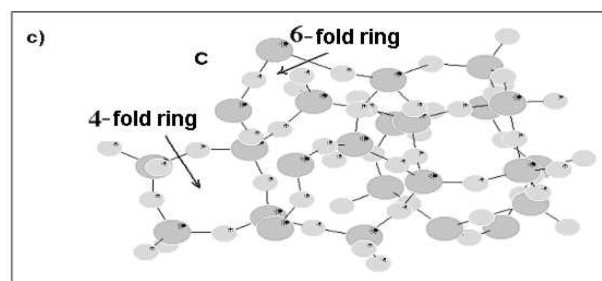

Fig. 2. *a* — position of the peak of the principal IR absorption zone as a function of the thickness of an oxide film; *b, c* — fragments of the SiO_2 structures formed by SiO_4 tetrahedra for various thicknesses

The results of the decomposition of the absorption band of ultrathin SiO_2films of various thicknesses are shown in Fig. 4. In the case of oxide layers thicker than 7 nm, the parameters of the both elementary bands (the positions of the maxima — 1050 and 1085 cm^{-1} , FWHM — 45 and 60 cm^{-1}, respectively) correlate rather well with those obtained in earlier works [13,14,23—25] for thermal SiO_2 films. In the case of oxide layers thinner than 7 nm, these parameters are strongly different: the first band becomes narrower ($H \approx 40$ cm^{-1}) and shifts towards the low-frequency region ($W \approx 1035$ cm^{-1}). An elementary band with such parameters is inherent to nonstoichiometric oxide films [25]. Hence, these data seem to have a certain physical sense (especially taking

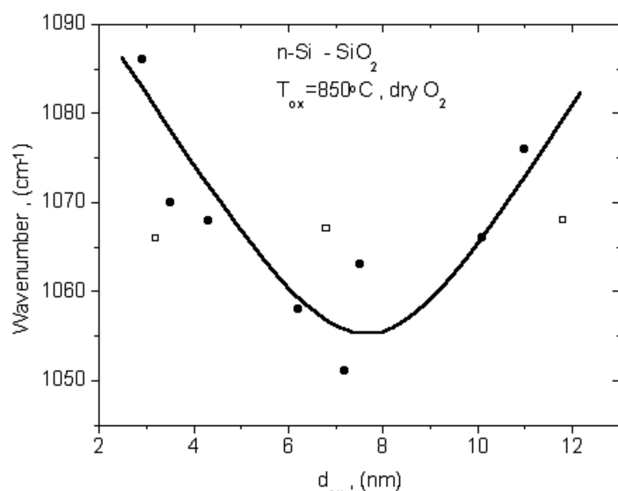

Fig. 3. Position of the maximum of the IR absorption spectrum as a function of the thickness of an silicon dioxide film (• — our results; □ — [19])

into account that, along with data obtained from IR spectra, the other oxide characteristics also change in the range of thicknesses less than 7 nm).

The structure of oxide films thicker than 7 nm is clear in principle and may be described as a mixture of 4- and 6-fold interconnecting rings. Vibrations of oxygen atoms lead to the appearance of two bands with the positions of maxima of 1050 and 1085 cm^{-1} (Fig. 4). As one can see from Fig. 4, the structure of oxide films thinner than 7 nm must be somewhat different. A decrease in the vibration frequency of oxygen atoms is conditioned by a reduction of the Si—O—Si angle. In a film of the stochiometric composition, such a decrease of the angle can be associated with a large distortion of 4-fold SiO_2 rings and/or with the appearance of a sufficient amount of 3-fold rings in the lattice of the thinnest oxides. On the other hand, the contribution of the band with $W = (1035 \pm 3)$ cm^{-1} and $H = (47 \pm 7)$ cm^{-1} is inherent to the Si—O stretching band of SiO_x films and is related to Si—O_2—Si_2 molecular clusters [25]. Thus, one can suppose that the structure of the thinnest oxides along with the rings formed by SiO_2 tetrahedra includes some amount of weakly oxidized silicon. To make a certain conclusion, it is necessary to carry out more detailed experiments using techniques sensitive to the structure.

The results obtained during our study of the structure of ultrathin silicon dioxide films have developed the existing knowledge about amorphous SiO_2 films. They are in good agreement with the fact of a significant spread of the Si—O—Si angles: from 120° to 180° with the peak of the distribution lying at 144° for thicker films [26]. The shift of the peak towards higher frequencies testifies to the strengthening of atomic bonds in silicon-oxygen $SiO_{4/2}$tetrahedra. A theoretical analysis of the structure of amorphous SiO_2 performed in [27] has shown the possibility for a middle- or far-range order to exist in the SiO_2 structure, in addition to the short-range order.

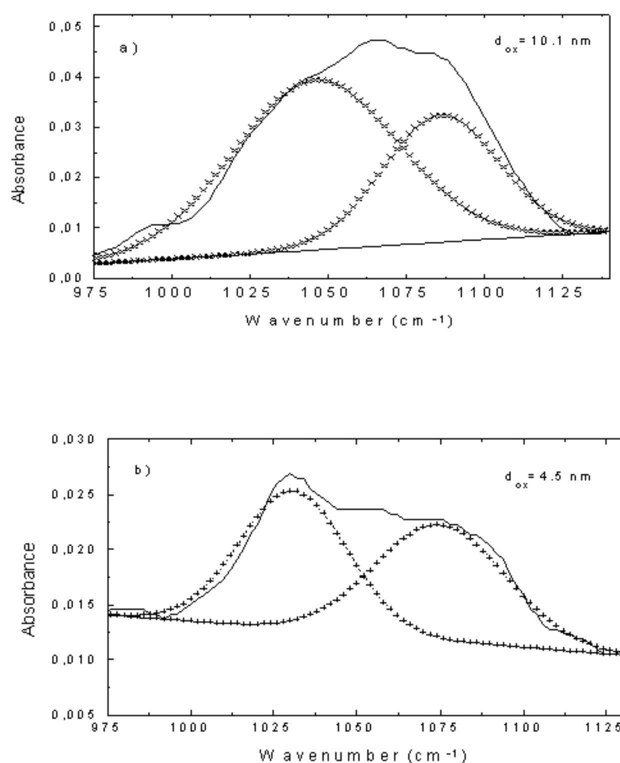

Fig. 4. Deconvolution of the principal IR absorption band of ultrathin SiO_2 films

E l l i p s o m e t r y. The refraction index n represents an important optical characteristic of SiO_2films. As was observed in [28], an increase of n accompanies a reduction of the thickness of a SiO_2film grown thermally on silicon up to the values lower than 10 nm. The results of ellipsometric measurements are interpreted by considering the complex values of the refractive indices of the substrate, $n_s^* = n_s^* - ik_s$, and the film, $n_f^* = n_f^* - k_f$, and are defined by the film thickness d_f. Ellipsometric measurements give a set of two parameters Ψ, Δ that characterize a variation of the polarization of light as it reflects from the surface

$$R_p/R_s = \text{tg}\Psi \exp(i\Delta), \quad (1)$$

where R_p and R_s are the complex refraction coefficients for light polarized in parallel and normally to the beam

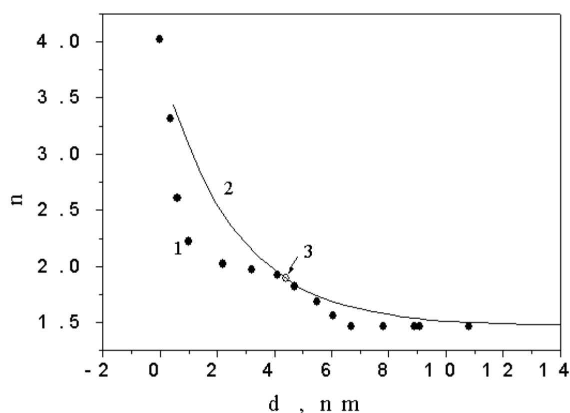

Fig. 5. Thickness dependence of the refractive index of a SiO_2 film: dark points — experiment; solid curve presents the dependence constructed according to $n = 1.465 + 2.4\exp(-3.913 \times 10^{-1}\ d)$ [25]; *3* — experimental point from [25]

incidence plane (the Fresnel coefficients). For transparent films, Δ and Ψ are cyclic functions of the oxide thickness. These data allow one to determine only two of the mentioned five parameters.

In order to increase the number of parameters that can be determined, one performs independent ellipsometric measurements that can be divided in three groups:

— Measurements on different wavelengths of light radiation (spectral ellipsometry).

— Multiple measurements with the controlled variation of one of the phases of the system. In this group, the most widely used measurements are those performed at a continuous increase (decrease) of the thickness of the upper layer of the system. In this case, it is considered that the characteristics of the rest of the layers remain constant.

— Many-angle measurements. In this group, with a necessary number of measurements performed at various angles of light incidence, it is possible to calculate the optical parameters of all layers of the investigated system.

The ellipsometric parameters Δ and Ψ can be determined with high accuracy, which makes ellipsometry one of the most sensitive methods for measurements of the film thickness.

In some cases, while determining the thickness and refractive index of a silicon-based SiO_2 film, we simplified the analysis of ellipsometric data. It was considered that SiO_2 films are completely transparent, that is $k_f = 0$. In addition, ellipsometry cannot be used for the determination of the imaginary part of the complex refraction index of the substrate k_s if the silicon surface is not atomically pure. This is conditioned by the fact that both a change in the magnitude of k_s and the presence of an ultrathin oxide film cause a shift only in the value of Δ, which can be considered as a part of the experimental error. In our experiments, a simplified analysis was carried out using the value $k_s = 0.00685$ obtained from the optical experiments on light transmission [29]. On the other hand, small changes of the real part of the refraction index of silicon n_s practically cause only a shift of Ψ. All these approaches decrease the number of the unknown parameters of materials to three: n_s, n_f, d_f. The analysis of the relationship between these parameters and ellipsometric data (Δ, Ψ) shows that, with decrease in the thickness of the film d_f, the influence of n_s increases. Thus, at a fixed value of n_s and small values of d_f, it is impossible to accurately determine n_f. At the same time, there is some inaccuracy in the determination of d_f.

The accurate determination of the parameters was performed at the successive growing or etching of a SiO_2 film in the range 0.5—20 nm. In this case, in the first stage, we measured the ellipsometric parameters of the film of a certain thickness without assigning the magnitude of n_s. After that, the thickness of the film increased (due to the growing) or decreased (due to etching) by a certain value, and the ellipsometric parameters Δ and Ψ were determined again. It was considered that the grown layer is uniform in thickness. The set of ellipsometric data gave a possibility to obtain the values of n_s, n_f, and d_f once more. At the following measurement of the parameters, we used the values of n_s from the previous measurement, and the value of n_f was determined accurately. This method gives a possibility to determine the distribution of the optical parameters of SiO_2 films over their thickness.

In Fig. 5, the dependence of n_f on d_f is depicted. The volume value of n_s was determined after the complete etching of a SiO_2 film and amounted to 3.865 ± 0.015. As one can see from Fig. 5, the Si—SiO_2 system is heterogeneous and consists of the half-infinite substrate and three layers that differ in the refractive index and are separated from one another with transition layers. The value of the refractive index $n = 3.9 \div 4.1$ can be related to the silicon substrate. Between silicon and the SiO_2 film, there exists a transition SiO_x layer. The thickness of this layer (1.5 nm) agrees well with the literature data that indicate the presence of a transition layer approximately 1 nm in thickness between silicon and SiO_2 [30—38]. The SiO_2 film is also heterogeneous

and includes two layers characterized with different refractive indices. The first layer has the parameters $d \approx (2 \div 3)$ nm and $n = 1.8 \div 2.0$ while the second one — $d > 8$ nm and $n = 1.46$. Between these two layers, there is a transition layer 3—5 nm in thickness.

An increase in n with a reduction of the growth temperature of SiO_2 is also observed. The investigations of the interrelation between the refractive index and the growth temperature performed in [39, 40] show that, with increase in T, the magnitude of n decreases up to 1.460. The SiO_2 films grown in dry O_2 are characterized by $n = 1.460$ at $T = 1150 \div 1200$ °C, and a further increase in T does not result in the variation of the refractive index. It is equal to n of pure fused quartz without mechanical stresses [41], i.e. the value of $n = 1.460$ represents the refractive index of a completely relaxed SiO_2 film [42]. A similar dependence of n on the oxidation temperature is also observed in the case of the growth of SiO_2 films in water vapors. In this case, a transition to constant values of n takes place at lower temperatures ($T = 1025$ °C) [40]. The annealing of SiO_2 in the nitrogen atmosphere at temperatures higher than the oxidation one results in a reduction of the refractive index. In this case, the value of n never becomes lower than that of fused quartz.

There is a correlation between the refractive index and the density ρ of SiO_2 films of the stoichiometric composition without impurities, which can be expressed [43] by the Gladstone—Dale ratio

$$\rho = K_1(n - 1) \tag{2}$$

or by the Lorenz—Lorentz formula

$$\rho = K_2(n^2 - 1)/(n^2 + 2), \tag{3}$$

where K_1 and K_2 are constants. K_1 is equals to 5.602 for the glass modifications of SiO_2, while $K_1 = 4.875$ for low-temperature crystal modifications and ordinary quartz glass.

Figure 6 shows the dependence of the density of a SiO_2 film on its thickness calculated according to Eqs. (2) and (3) on the basis of the experimental results which we obtained for n. For the ρ(d) dependence, one can observe that ρ decreases with the thickness of SiO_2 films. For films thinner than 6 nm, incredibly high values of the density were obtained, which is conditioned by the incorrectness of using Eqs. (2) and (3) in this range of thicknesses due to the existence of a silicon-enriched SiO_2 layer near the Si/SiO_2 interface. The highest density of SiO_2 films obtained experimentally amounted to 2.70 g/cm^3 [44]. At the same time, it is

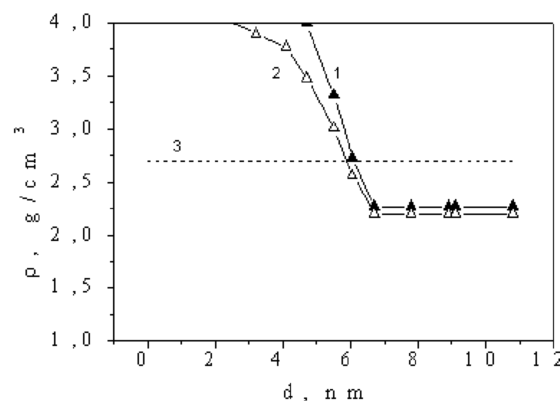

Fig. 6. Dependences of the density of thin SiO_2 films on their thickness calculated according to experimental data on the thickness dependence of the refractive index *1* — according to Gladstone—Dale equation; *2* — from Lorenz—Lorentz equation; *3* — the level of the highest densities measured experimentally

worth noting that the detailed experimental investigation of the thickness dependence of the density revealed a non-monotonous character for films grown at $T = 1000$ °C [44]. In thermal SiO_2 films grown at temperatures lower than 1000 °C, one observes a significant increase of both the oxide density [39,45] and internal mechanical stresses [46—48].

The main reason of an increase in the density of ultrathin SiO_2 films is the presence of high compressive stresses in them near the Si—SiO_2 interface [49, 50], whose magnitude increases with a reduction in the oxidation temperature. For example, a considerable increase of the density of films up to $\rho = 2.31$ g/cm^3 at $T = 900$ °C was observed in [51]. A growth of the density at low temperatures is associated with a sharp increase of mechanical stresses due to a rise in the viscosity of silicon dioxide with decrease in temperature as well as a significant (approximately by a factor of 2.2) growth of the molar volume that accompanies the oxidation of silicon to SiO_2. At low oxidation temperatures, the viscosity of the oxide becomes so large [51] that the time of relaxation of internal stresses at the expense of a viscous spreading is significantly larger than the oxidation time. In this case, the stressed state is maintained for an indefinitely long time, and the film density increases. At high oxidation temperatures, when the time of relaxation of stresses is significantly lower than the oxidation time, the volume of films increases due to the viscous spreading, mechanical stresses decrease, and the density of thermal SiO_2 films corresponds to the values for vitreous SiO_2. A

viscoelastic model that describes the generation of stresses at the Si—SiO_2 interface due to the difference of Si and SiO_2 molar volumes [47,52—54] displays a viscoelastic flow of SiO_2 normally to the surface. At a given temperature, the oxide film will rearrange oneself as soon as the viscosity allows. The model also foresees a gradient of mechanical stresses (and, hence, of the density) which decreases in the direction from the Si—SiO_2 interface to the SiO_2 surface. However, the appearance and the relaxation of mechanical stresses are significantly more complicated processes than it can be described by a simple viscoelastic model. Intrinsic stresses in a SiO_2 film obtained by means of the oxidation of silicon at 973 °K amount to approximately 4×10^8 Pa. At T = 1423 K, they practically disappear, and residual stresses are determined solely by the discrepancy of the thermal expansion coefficients of silicon (4.5×10^{-6} K^{-1}) and SiO_2 (0.6×10^{-6} K^{-1}) [51]. Investigations of properties of the densification under the action of high pressures (higher than 10^{10} dyn/cm^2) of the volumetric silicon dioxide have shown that, under the variation of the refraction coefficient from 1.459 to 1.472, the film density increases by 2—3%. An increase of the film thickness by approximately 3% accompanying the relaxation of mechanical stresses in the Si—SiO_2 system was observed in [54] during a successive thermal annealing in an inert atmosphere. In contrast to other inorganic solid bodies, glass can be continuously densified under the influence of high pressures, moreover, the densification increases with temperature and pressure. In the process of densification, in parallel to a rise in the density, there also occur variations of other properties such as the refractive coefficient, chemical resistance, microhardness, etc. X-ray investigations of quartz glass [55, 56] have shown that the densification occurs due to the variation of Si—O—Si angles without a break and variation of the length of Si—O bonds.

The analysis of elastic stresses in the Si—SiO_2 system [57] demonstrates that the model allowing for a sharp interface between silicon and its oxide doesn't correspond to experimental facts. Instead, it is necessary to suppose the existence of a certain interface layer at the Si—SiO_2 interface, in which there occurs the compensation of a part of mechanical stresses appearing in the system.

An important problem arising in the investigations of ultrathin SiO_2 films is the clarification of peculiarities of the structural and chemical transitions from crystalline silicon (c-Si) to amorphous SiO_2 (a-SiO_2). Various experiments indicate the existence of a transition layer narrower than 1 nm, moreover, the microcrystallinity was revealed near the interface [58]. The ion channeling has shown that, within 0.5 nm, Si atoms in SiO_2 are arranged in a definite order with respect to the substrate [59]. The method of high-resolution transmission electron microscopy allowed one to reveal the existence of an epitaxial oxide, being several atomic layers in thickness [60]. In [61], the presence of an epitaxial transition layer less than 0.5 nm in thickness was revealed with the help of experiments using the method of X-ray dispersion at a grazing incidence.

The results, which we obtained in the course of investigations of the properties of SiO_2 films grown at low temperatures (<1000 °C) in dry O_2 by IR spectroscopy and ellipsometry indicate an increase of the refractive index and a decrease of the frequency of IR oscillations of the bonds for the films obtained at temperatures lower than 1000 °C. It is shown that the systematic and correlated changes of the refractive index and the frequency of IR oscillations result from an increase of the film density due to a decrease in the SiO_2 thickness and the growth temperature. Variations of n, ν_m, and ρ are explained in terms of a decrease of the Si—O—Si angle of silicon-oxygen tetrahedra. A decrease of the Si—O—Si angle results in a decrease of the Si—Si distance. The film density is proportional to the Si—Si distance.

E t c h i n g. Measurements of the refraction coefficient and the etching rate performed at the etching of SiO_2 films grown by different methods give a possibility to obtain information about the film composition, bond strength, deviation from the stoichiometric composition, as well as the density and porosity. The etching rate of quartz glass decreases with increase in its density. It is known that the crystalline modification of SiO_2 with a density of 2.93 g/cm^3 and n = 1.594 (coesite) stable at high pressures practically doesn't dissolve in concentrated hydrofluoric acid at room temperature [62].

When determining the thickness dependence of the etching rate, the step-by-step etching of SiO_2 was performed in a water solution of hydrofluoric acid (HF:H_2O=1:100 and HF:H_2O=1:25). The thickness of a SiO_2 film grown at T = 800 °C in dry O_2 on n-type silicon with the substrate orientation (111) as a function of the etching time is depicted in Fig. 7. As one can see, the etching rate (the slope of the $d(t_{\rm et})$ function) depends on the film thickness. SiO_2 layers thinner than 4 nm have lower etching rates, which correlates with a higher density of the SiO_2 layer adjacent to silicon [21, 44] caused by the coesite-like structure of the film and

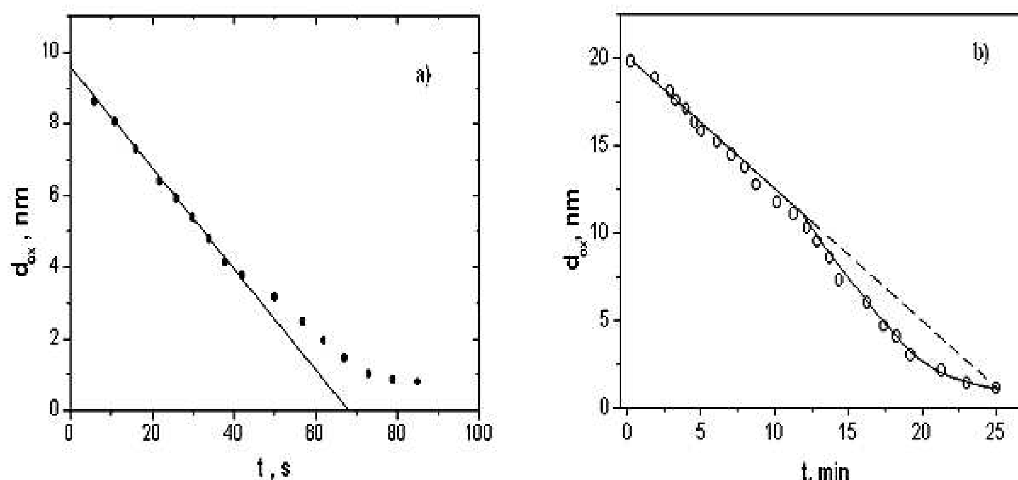

Fig. 7. Etching kinetics of a SiO_2 film in a water solution of hydrofluoric acid of various concentrations: *a* — HF:H_2O= 1:25; *b* — HF:H_2O= 1:100

compressive stresses. In the transition region (∼5 nm) where the film structure changes, one observes a higher etching rate as compared to ν_{et} of upper SiO_2 layers. It is caused by the weakening of bonds in the film as a result of the structural reconstruction. This fact indicates a significant distinction in the structures of the SiO_2 layer adjacent to the silicon substrate and the distant one.

4. Conclusions

We have discovered the nonmonotonous dependences of the positions of maxima of IR spectra, the refractive index, and the etching rate on the thickness of SiO_2 films. The obtained results confirm the data on the layered structure of silicon dioxide films. The position of the IR spectra maximum reaches a minimal value at d ≈7 nm, while the etching rate increases in the neighborhood of this value. That fact indicates the weakening of chemical bonds. The thickness of 7 nm corresponds to the transition region from a coesite-like structure of SiO_2 films to a tridymite-like one.

1. *Green M.L., Gusev E.P., Degraeve R., Garfunkel E.L.* // J. Appl. Phys.— 2001.—**90**, N5.— P.2057.
2. *Depas M., Heyns M.M., Nigam T. et al.* // Proc. 3rd Intern. Symp. on the Phys. and Chem. of SiO_2 and the Si—SiO_2 Interface.— Pennington: The Electrochem. Soc. Inc., 1996.— Vol.3.— P.350.
3. *SIA 1994* National Technology Roadmap for Semiconductors.— (Semiconductor industry association, 1994).
4. *Tiwari S.* // Proc. 3rd Intern. Symp. on the Phys. and Chem. of SiO_2 and the Si—SiO_2 Interface.— Pennington: The Electrochem. Soc. Inc., 1996.— Vol.3.— P.250.
5. *Tiwari S., Rana F., Hanafi H. et al.* // Appl. Phys. Lett.— 1996.— **68**, N10.— P.1377.
6. *Fukudla M., Nakagawa K., Miyazaki S., Hirose M.* // Ibid.— 1997.— **70**, N17.— P.2291.
7. *Ammendola G., Vulpio M., Bileci M. et al.* // J. Vac. Sci. and Technol.— 2002.— **B20**, N5.— P.2075.
8. *Fukuda H., Endoh T., Nomara S.* // Proc. 3rd Intern. Symp. On the Phys. And Chem. of SiO_2 and the Si—SiO_2 Interface.— Pennington, NJ, USA: The Electrochem. Soc. Inc., 1996.— Vol.3.— P.15.
9. *Tu Y., Tersoff J.* // Thin Solid Films.— 2001.— **400**.— P.95.
10. *Litovchenko V.G., Gorban' A.P.* The Foundations of the Metal–Dielectric–Semiconductor Systems of Microelectronics. — Kyiv: Naukova Dumka.— 1978 (in Russian).
11. *Litovchenko V.G.* The Foundations of the Physics of Semiconductor Layered Systems.– Kyiv: Naukova Dumka, 1980 (in Russian).
12. *Litovchenko V.G., Popov V.G., Evtukh A.A.* // Appl. Surf. Sci.— 1989.— **39**.— P.238.
13. *Lisovskii I.P., Litovchenko V.G., Lozinskii V.B., Steblovsky G.I.*// Thin Solid Films.— 1992.— **213**.— P.164
14. *Lisovskii I.P., Litovchenko V.G., Khatko V.V.*// Microelectron. Eng.— 1993.— **22**.— P.39.
15. *Graf D., Grundner M., Schulz R., Muhlhoff L.*// J. Appl. Phys.— 1990.— **68**.— P.5155.
16. *Borghesi A., Sassella A.* // Phys. Rev. B.— 1994.— **50**.— P.17756.
17. *Sassella A., Pivac B., Abe T., Borghesi A.* // Mater. Sci. and Eng. B.— 1995.— **36**.— P.221.
18. *Pliskin W.A., Guall R.P.* // J. Electrochem. Soc.— 1964.— **111**, N7.— P.872.
19. *Boynd I.W., Wilson J.I.B.* // J. Appl. Phys.— 1987.— **62**, N8.— P.3195.

20. *Boynd I.W., Wilson J.I.B.* // Appl. Phys. Lett.— 1987.— **50**, N5.— P.320.

21. *Litovchenko V.G., Evtukh A.A., Lisovskii I.P. et al.* // Ukr. Fiz. Zh.— 1998.— **43**.— P.607.

22. *Martinet C., Devine R.A.B.*// J. Non-Cryst. Solids.— 1995.— **187**.— P.96.

23. *Boyd I.W.*// Appl. Phys. Lett.— 1987.— **51**.— P.418.

24. *Garrido B., Samitier J., Moranonte J.R. et al.*.// Appl. Surf. Sci.— 1992.— (**56—58**).— P.861.

25. *Lisovskii I.P., Litovchenko V.G., Lozinskii V.B. et al.* // J. Non-Cryst. Solids.— 1995.— **187**.— P.91.

26. *Revesz A.G.* // Phys. status solidi (a).— 1980.— **57**, N1.— P.235.

27. *Lehmann A., Schumann L., Hubner K.* // Phys. status solidi (b).— 1983.— **117**, N2.— P.689.

28. *Hebert K.J., Labayen T., Irene E.A.* // Proc. 3rd Intern. Symp. on the Phys. and Chem. of SiO_2 and the Si—SiO_2 Interface.— Pennington: The Electrochem. Soc. Inc., 1996.— Vol.3.— P.81.

29. *Van der Meulen Y.J.* // J. Electrochem. Soc.— 1972.— **119**, N4.— P.530.

30. *Barsony J., Giber J.* // Appl. Surf. Sci.— 1980.— **13**, N2.— P.1428.

31. *Krivanek O.L., Tsui D.C., Shend T.T., Kangar A.* // Proc. Intern. Top. Conf. "Phys. SiO_2 and its Interfaces".— Yorktown Heights, N.Y, 1978.— P.356.

32. *Krivanek O.L., Mazur J.H.* // Appl. Phys. Lett.— 1980.— **37**, N4.— P.392.

33. *Goodnik S.M., Grann R.G., Ferry O.K.et al.* // Surf. Sci.— 1982.— **113**, N1.— P.233.

34. *Aspens D.E., Theen J.B.* // Phys. Rev. Lett.— 1979.— **43**, N14.— P.1046.

35. *Distefano T.H.* // Proc. Intern. Top. Conf. "Phys. SiO_2 and its Interfaces".— Yorktown Heights, N.Y., 1978.— P.362.

36. *Derrien J., Commandre M.* // Surf. Sci.— 1982.— **118**, N1/2.— P.32.

37. *Jackman T.E., MacDonald J.R., Feldman L.C. et al.* // Surf. Sci.— 1980.— **100**, N1.— P.35.

38. *Green M.L., Gusev E.P., Degraeve R., Garfunkel E.L.* // J. Appl. Phys.— 2001.— **90**, N5.— P.2057.

39. *Taft E.A.* // J. Electrochem. Soc.— 1978.— **125**, N6.— P.968.

40. *Taft E.A.* // Ibid.— 1980.— **127**, N4.— P.993.

41. *Malitson I.H.* // J. Opt. Soc. Amer.— 1965.— **55**, N — P.1205.

42. *Landsberger L.M., Tiller W.A.* // Appl. Phys. Lett.— 1986.— **49**, N3.— P.143.

43. *Pliskin W.A.* // J. Vac. Sci. and Technol.— 1977.— **14**, N5.— P.1064.

44. *Lisovski I.P., Litovchenko V.G., Lozinski V.B. et al.* // Proc. 3rd Intern. Symp. on the Phys. and Chem. of SiO_2 and the Si—SiO_2 Interface.— Pennington: The Electrochem. Soc. Inc., 1996.— Vol.3.— P.592.

45. *Irene E.A., Dong D.W., Zeto R.J.* // J. Electrochem. Soc.— 1980.— **127**, N2.— P.396.

46. *Kobeda E., Irene E.A.* // J. Vac. Sci. and Technol. B.— 1986.— **4**, N3.— P.720.

47. *Eernisse E.P.* // Appl. Phys. Lett.— 1979.— **35**, N1.— P.8.

48. *Eernisse E.P.* //Ibid.— 1977.— **30**, N6.— P.290.

49. *Brozek T., Kiblik V.Ya.* // Optoelectronics and Semiconductor Technique. — 1992. — N22. — P.53.

50. *Giber J., Deak P., Marton D.* // Phys. status solidi (b).— 1977.— **79**, N3.— P.K89.

51. *Irene E.A., Tierney E., Agilello I.* // J. Electrochem. Soc.— 1982.— **129**, N11.— P.2594.

52. *Irene E.A., Teirneg E., Anzeillo J.* // Ibid.— P.2594.

53. *Tiller W.A.* // Ibid.— 1980.— **127**, N3.— P.619.

54. *Tiller W.A.* // Ibid.— P.625.

55. *Mackenzie J.D.* // J. Amer. Ceram. Soc.— 1963.— **46**, N10.— P.461.

56. *Mackenzie J.D.* // Ibid.— 1964.— **47**, N2.— P.76.

57. *Jaccodine R.J., Schlegel W.A.* // J. Appl. Phys.— 1966.— **37**, N6.— P.2429.

58. *Fuoss P.H., Norton L.J., Brennam S., Fischer-Colbrie A.* // Phys. Rev. Lett.— 1988.— **60**, N7.— P.600.

59. *Cheung N.W., Feldman L.C., Silverman P.J., Stensgard I.* // Appl. Phys. Lett.— 1979.— **35**, N11.— P.859.

60. *Ourmazd A., Rentschler J.A., Bevk J.* //Ibid.— 1988.— **53**, N9.— P.743.

61. *Renaud G., Fuoss P.H., Ourmazd A. et al.* //Ibid.— 1991.— **58**, N10.— P.1044.

62. *Coes L.A.* // Science.— 1953.— **118**, N305— P.131.

Received 28.03.05.
Translated from Ukrainian by H. Kalyuzhna

ДОСЛІДЖЕННЯ СТРУКТУРИ НАДТОНКИХ ПЛІВОК ДВОХОКИСУ КРЕМНІЮ

А.А. Євтух, І.П. Лісовський, В.Г. Литовченко, А.Ю. Кизяк, Ю.М. Педченко, Л.І. Самотовка

Р е з ю м е

Детально досліджено структурні властивості надтонких (2—10 нм) і тонких (10—40 нм) плівок двохокису кремнію, термічно вирощених в атмосфері кисню на кремнії при $T = 800 \div 950$ °C. Структуру одержаних плівок було вивчено трьома незалежними аналітичними методами, а саме методами ІЧ-спектроскопії, еліпсометрії та покроковим хімічним травленням. Була виявлена широка перехідна область SiO_2, що прилягає до кремнію. Перехідна область між кремнієм і об'ємним SiO_2 є неоднорідною і складається з трьох шарів. Існує перехідний шар SiO_x завтовшки приблизно 1,5 нм між Si і SiO_2. Плівка SiO_2 є також неоднорідною і складається з двох шарів. Перший шар має товщину $d = 2 \div 3$ нм, а товщина другого — $d > 8$ нм. Між цими двома шарами існує перехідний шар завтовшки 3—5 нм.